Pakistan Veterinary Journal

ISSN: 0253-8318 (PRINT), 2074-7764 (ONLINE)
DOI: 10.29261/pakvetj/2026.008

RESEARCH ARTICLE

Comparative Proteomics Reveals Molecular Adaptations to High-Altitude Stress in Three *Hypoderma* Species

Shuai Wang[1], Zhi Li[1], Ru Meng[2*], Hong Duo[1], Xueyong Zhang[1], Xiuying Shen[1], Jing Li[3], Yuanqing Lin[3], Duojie Caidan[4], Xuhao Zeng[5], Wangkai Chen[5], Mikhlid H. Almutairi[6] and Yong Fu[1*]

[1]Academy of Animal Science and Veterinary, Qinghai Provincial Key Laboratory of Pathogen Diagnosis for Animal Diseases and Green Technical Research for Prevention and Control, State Key Laboratory for Diagnosis and Treatment of Severe Zoonotic Infectious Diseases, Key Laboratory for Zoonosis Research of the Ministry of Education, Qinghai University, 810016 Xining, China; [2]Xining Animal Disease Prevention and Control Center, 810016 Xining, China; [3]Animal Disease Prevention and Control Center of Qinghai Province, 810001 Xining, China; [4]Guoluo State Animal Disease Prevention and Control Center, Maqin 814000, China; [5]Agrichina Pharmaceutical Co., Ltd.; Qichun 435300, China; [6]Zoology Department, College of Science, King Saud University, P.O. Box: 2455, 11451, Riyadh, Saudi Arabia
*Corresponding author: qhfuyong@163.com; mr-0522@163.com

ARTICLE HISTORY (25-1145)

Received: November 15, 2025
Revised: December 14, 2025
Accepted: December 16, 2025
Published online: January 22, 2026

Key words:
2D-DIGE
Heat shock protein
High-altitude environment
Hypoderma
Proteomic
Qinghai-Tibet Plateau.

ABSTRACT

Warble flies (*Hypoderma* spp.) cause large financial losses to the livestock sector on the Qinghai-Tibet Plateau, but little is known about the molecular adaptations that enable them to survive at high elevations. A comparative proteomic analysis was conducted on third-instar larvae from three important species—*H. bovis*, *H. sinense*, and the endemic *H. pantholopsum*—was motivated by this knowledge gap. By integrating mass spectrometry and two-dimensional differential in-gel electrophoresis (2D-DIGE), a total of 54 differentially expressed proteins were identified, which were enriched in stress-response biomarkers such as heat shock protein HSC72 and HSP60, and predominantly exhibited acidic properties with isoelectric points ranging from 3.78 to 6.76, and differentially expressed ($P<0.05$). According to functional profiling, the main molecular functions were binding (39.4%) and catalytic activity (37.9%), with cellular and metabolic processes receiving a significant amount of attention (30.0% each). Only two proteins were found to be conserved across species, which was a startling discovery in contrast to the 41.5% of differential proteins that were specific to the *H. bovis* and *H. pantholopsum* pair. Comparative proteomic analysis demonstrated the upregulation of pathways associated with protein homeostasis and energy metabolism in *H. pantholopsum*, a species highly adapted to high-altitude habitats. Phylogenetic analysis of HSC72 uncovered functional conservation, indicating an adaptive response molded by long-term evolutionary processes. Collectively, our findings identify potential targets for future species-specific control strategies against hypodermosis on the Qinghai-Tibet Plateau, while also unraveling key molecular mechanisms that underpin the adaptation of these parasitic larvae to the extreme high-altitude environment.

To Cite This Article: Wang S, Li Z, Meng R, Duo H, Zhang X, Shen X, Li J, Lin Y, Caidan D, Zeng X, Chen W, Almutairi MH and Fu Y, 2026. Comparative proteomics reveals molecular adaptations to high-altitude stress in three *Hypoderma* species. Pak Vet J. http://dx.doi.org/10.29261/pakvetj/2026.008

INTRODUCTION

The average elevation of Qinghai Province, which is located in the northeastern Qinghai-Tibet Plateau, is higher than 3,000 meters. Yaks and Tibetan sheep are essential to the pastoral economy that thrives in this high-altitude setting. More than 4.8 million yaks graze on the pastures between 3,000 and 4,500 meters, where *Hypoderma* spp. are common parasites affecting these animals.(Pan *et al.*, 2024) Hypodermosis is a serious disease affecting livestock worldwide (Qing, 2022). Worldwide, *Hypoderma bovis* (*H. bovis*) and *Hypoderma lineatum* (*H. lineatum*) are the most common causes of bovine hypodermosis, a severe myiasis (Guan and Tai, 2023). However, *Hypoderma sinense* (*H. sinense*) is the main agent in Qinghai's yaks (Fu *et al.*, 2016). With an overall prevalence in yaks ranging

from 70 to 95% and reaching 100% in some regions, the extent of infection is astounding (Li *et al.*, 2014). Numerous other hosts are also infect the parasite, have wildlife such as Tibetan antelope (Ma and Ge, 2017), *Cervus elaphus* (González *et al.*, 2023), and plateau zokor (Hou, 2021). Occasional have reported in sheep, deer, and horses (Cairen *et al*., 2019). What's concerning is human infections have been found, particularly among nomadic herders with frequent yak contact (Zhang *et al.*, 2014). These reports confirm the parasite's serious zoonotic threat.

Hypodermosis is a subcutaneous myiasis, It can cause significant economic losses in the livestock industry (Li *et al.*, 2018). It can lead to reduced weight gain in cattle, decreased milk production, and deterioration of leather quality (Hassan *et al.*, 2010). The economic and zoonotic problems of warble flies are quite significant, no systematic control of measures against parasite infection have been applied in Qinghai Province. To establish a control method, we investigated the seasonal migration of *Hypoderma* larvae in yaks and different locations in the province and conducted a large-scale anthelmintic control program targeting first-stage larvae in four counties (Maqin, Yushu, Guinan and Haiyan counties) in Qinghai Province between 2008 and 2012.

Qinghai province covers a total area of over 721,000 km^2, stretching approximately 1200 km east-west and 800 km north-south, with an average elevation of over 3000 m above sea level. *Hypoderma bovis* and *H. sinense* were sampled from localities about Qinghai. For *H. bovis*, specimens were harvested in Maqin County (MQ), Haiyan County (HY), Huzhu County (HZ), Minhe County (MH) and Chengduo County (CD). For *H. sinense*, sampling sites were located in Maqin County (MQ), Guinan County (GN), Haiyan County (HY), Tanggula City (TGL), and Chengduo County (CD) (Fig. 1). The larvae of *Hypoderma pantholopsum* (*H. pantholopsum*) were collected at an elevation of 4,479 m from the Suonandajie Protection Station in Hoh Xil National Nature Reserve.

Currently, research on *Hypoderma* spp. in high-altitude regions is limited. Most existing studies focus on pathological reports (Shao and Yang, 2022), epidemiological surveys, and control strategies (Wang, 2025). Comparative analyses between different species and proteomic studies are relatively scarce. Therefore, this study aims to compare the proteomes of three *Hypoderma* species to identify differentially expressed proteins, thereby elucidating the mechanisms underlying their adaptation to high-altitude environments.

MATERIALS AND METHODS

Main reagent: The reagents provided by GE Healthcare (USA) and their corresponding catalog numbers are as follows: IPG buffer (pH4～7) (17600086), Cy2 fluorescent dye (PA22000), Cy3 fluorescent dye (PA23000), and Cy5 fluorescent dye (PA25000); CHAPS (Catalog No. 1610460) and DTT (Catalog No. 1610610) were purchased from Bio-Rad Laboratories, Inc. (Hercules, CA, USA). Tris base (T8060) and EDTA disodium salt (E8040) were purchased from Solarbio Science & Technology Co., Ltd. (Beijing, China). The reagents provided by Sigma (USA) and their corresponding catalog numbers are: Molecular Weight Marker (17-0446-01), Polyvinylpolypyrrolidone

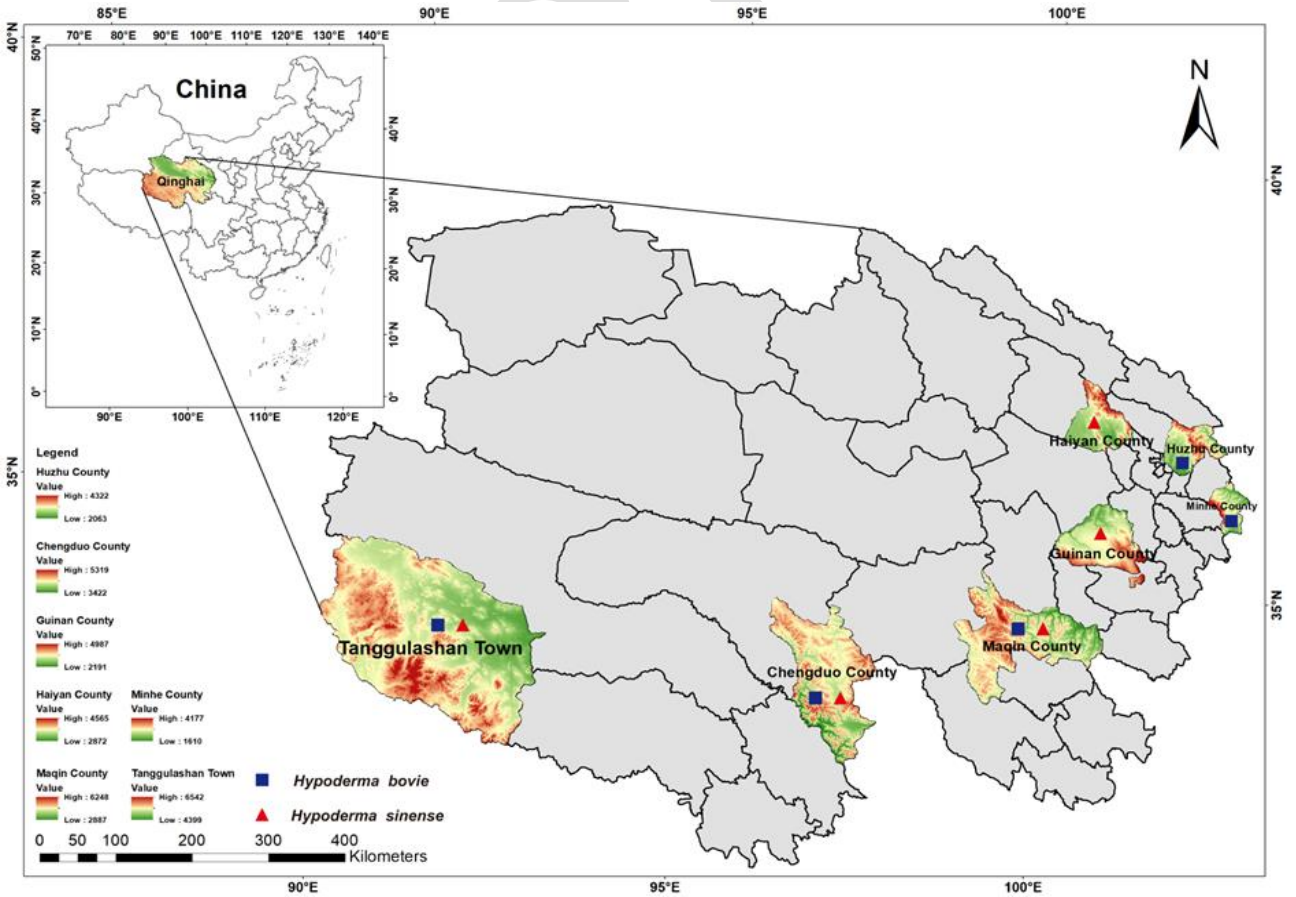

Fig. 1: Geographical distribution of warble fly collection sites.

(PVPP) (P6755), bovine serum albumin (BSA) (A7906), L-lysine (L8662), Urea (U5378), Thiourea (T7875), sodium dodecyl sulfate (SDS) (L4390), and α-cyano-4-hydroxycinnamic acid (C2020); Borax (catalog number BG12) is supplied by Guangzhou Chemical Reagent Factory (China); Trypsin (03708985001, sequencing-grade modified trypsin) is provided by Roche (Switzerland). All other chemical reagents were purchased from Beijing Chemical Reagent Company.

Sampling strategy: From 2013 to 2014, we collected 60 third-stage *H. bovis* larvae and 52 third-stage *H. sinense* larvae in Qinghai Province, 12 third-instar *H. pantholopsum* were collected at Suonandajie Protection Station in Hoh Xil National Nature Reserve. Initial differentiation of *H. bovis* and *H. sinense* relied on morphological traits (Li, 2007), later validated by COI gene analysis (Hebert *et al.*, 2003; Weigl *et al.*, 2010). Some samples were fixed by immersion in 70% ethanol, while the others were kept in -70ºC ultra-low temperature refrigerator. The sample size satisfies the criteria for routine experimentation. The three samples were designated as HS, HB, and HP.

Protein extraction: Total proteins were extracted by the Borax/PVPP/Phenol (BPP) protocol (Wang *et al.*, 2022). Briefly, all third-instar *Hypoderma* larval samples were processed individually, with each sample being washed three times using BPP buffer. (100 mM Tris, 100 mM EDTA, 50 mM borax, 50 mM vitamin C, 1% PVPP w/v, 1% Triton X-100 v/v, 2% b-mercaptoethanol v/v, 30% sucrose w/v, pH 8.0), approximately 1 g of sample was added to 10 mL ice-cold BPP buffer and completely ground to a slurry with a mortar and pestle on ice. The sample was then vortexed and two volumes of Tris-saturated phenol (pH 8.0) were added, followed by further vortexing for 10 minutes. The mixture was centrifuged at 16,000g for 15 minutes at 4ºC. The suspension was transferred to 50 mL centrifuge tubes, an equal volume of BPP buffer was added, and the mixture was vortexed for 5 minutes. After centrifugation (4 ºC, 15 min, 16,000 g), the suspension was transferred to a new centrifuge tube and five volumes of ammonium sulfate saturated methanol were added and incubated at -20 ºC overnight. The precipitated material was collected by centrifugation as described above. The protein pellet was washed with ice-cold methanol, followed by two washes with chilled acetone under the same centrifugation conditions (4 ºC, 15 min, 16 000 g). Finally, the suspension was discarded and the washed pellet was air-dried, then approximately 1 g of the air-dried pellet was lysed in 1 mL lysis buffer (7 M urea, 2 M thiourea, 2% CHAPS, 13 mM DTT, 1% IPG buffer) at 22 ºC for at least 2 hours. After centrifugation (20 ºC, 30 min, 20000 g), the suspension was filtered through a 0.22 μm filter and transferred separately into 1.5 mL centrifuge tubes. Protein concentration was determined by the Bradford assay using bovine serum albumin (BSA) as a standard and stored at -80°C until use.

2-D DIGE analysis: 2D-DIGE was used to analyze protein samples from three *Hypoderma* larvae (Li *et al.,* 2011). For each sample, 50μg of protein was taken randomly and labeled with 400 pmol of either Cy3 or Cy5 fluorescent dye (GE Healthcare, USA). An internal standard was prepared by pooling an equal amount of each sample and labeling with 400 pmol of Cy2. The labeling reaction was carried out on ice in the dark for 30 min and subsequently quenched with 10 mM lysine for 10 min. The three labeled samples were then combined and adjusted to a volume of 450μL using rehydration buffer (7 M urea, 2 M thiourea, 2% CHAPS). Next, 5μL of IPG buffer (GE Healthcare, USA) was added, and the mixture was centrifuged prior to isoelectric focusing (IEF). IEF was performed using 24 cm immobilized pH gradient (IPG) strips with a linear pH range of 4–7 under the following conditions: 250 V for 3 h, 500 V for 2 h, 1000 V for 1 h, a gradient increase to 8000 V over 3 h, and finally holding at 8000 V until a total of 110,000 Vh was reached. The second-dimension separation was conducted using 12.5% SDS-PAGE.

Gel scanning and image analysis: The Cy2-, Cy3-, and Cy5- labeled images were scanned with a Typhoon Trio scanner (GE Healthcare, USA), and the 2-D DIGE images were analyzed using DeCyder 6.0 software package (version 6.04.11, GE Healthcare) (Dowling, 2023). The differential in-gel analysis module was used for spot detection, and the biological variation analysis module was then used to detect the differentially expressed protein spots (confidence above 95%) with a fold change > 1.2 and statistical significance at $P < 0.05$. Three biological replicates were conducted in each comparison to ensure the protein spots' reproducibility.

MALDI-TOF MS analysis and database search: In this paper, the protein spots showing differential expression were manually resected, and then the gel digestion operation was carried out using trypsin according to the determined protocol (Mansuri *et al.*, 2024; Tsuchida *et al.*, 2020). After that, the obtained tryptophan peptide was mixed with the saturated solution of α -cyano-4-hydroxycinnamic acid in a 1:1 ratio and labeled on the MALDI target plate. In mass spectrometry analysis, the Mascot search parameters are set as follows: the database selected is NCBI nr (210.0); the digestion enzyme is Trypsin/P, allowing up to one missed cleavage site; the fixed modification is Carbamidomethyl (C), and the variable modification is Oxidation (M); the peptide tolerance is set to 300 ppm, and the MS/MS tolerance is 0.3 Da; the peptide charge states include 1+, 2+, and 3+; the data format is Mascot generic, and the instrument type is MALDI-TOF-TOF (Applied Biosystems, USA). To identify proteins, the obtained mass spectra were then processed and compared to the NCBInr database using the MASCOT search engine (http://www.matrixscience.com) (Zhang and Chait, 2000).

Bioinformatics: Sequences from the minimal list of proteins were retrieved from the UniProt (2016_04) database and scanned for signal peptide prediction and subcellular localization using SignalP 5.0 (Almagro Armenteros *et al.*, 2019), TargetP 1.1(Emanuelsson *et al.*, 2007), and SecretomeP 2.0 (Bendtsen *et al.*, 2004). Gene Ontology (GO) annotation was performed using Blast2GO(Kumar, 2025). Annotation enrichment was achieved via ANNEX and integration of GO terms linked to functional domains identified through InterPro 60.0

database scans (Blum *et al.*, 2021). The statistical framework DAVID (Huang, Sherman, and Lempicki, 2009) was used to identify statistically enriched GO terms associated with sex- or stage-specific secreted proteins compared to the GO terms associated with the complete set of identified proteins. Contingency tables were generated for each GO term in the test group and P values were calculated using Fisher's exact test. P values were adjusted for multiple testing by calculating the false discovery rate and the family-wise error rate.

RESULTS

Conserved protein diversity and species-specific expression patterns in *Hypoderma* larvae revealed by integrated SDS-PAGE and 2D-DIGE proteomics: Analysis of total proteins from the three *Hypoderma* larval species by SDS-PAGE revealed that the protein samples were of high quality and well-suited for the ensuing analytical steps.

In the gel-to-gel analysis, pairwise comparisons were conducted among the three *Hypoderma* species, specifically between *Hypoderma bovis* and *Hypoderma sinense* (designated as HB/HS), *Hypoderma bovis* and *Hypoderma pantholopsum* (designated as HB/HP), and *Hypoderma sinense* and *Hypoderma pantholopsum* (designated as HS/HP). More than 1031 spots were detected on each CyDye-labeled gel in the pH range of 4-7. The differential expression proteins in three experimental groups were separated use two-dimensional differential in-gel electrophoresis (2D-DIGE) technology. All samples distributed across three fluorescent gels (May *et al.*, 2021; Robotti and Marengo, 2018). Fig. 2(B-D) showed the fluorescence-labeled differential gel electrophoresis images. On the left side of the fluorescent electrophoretograms, the Cy2-, Cy3-, and Cy5-labeled images are sequentially arranged from top to bottom under their respective excitation/emission wavelengths. Fig. 2-E illustrates the overall protein differential spots across the three samples.

Targeted identification of differentially expressed proteins by MALDI-TOF MS: A total of 54 DEPs were confirmed across the three pairwise comparisons of *Hypoderma* species (*H. bovis* vs *H. sinense*, *H. bovis* vs *H. pantholopsum*, *H. sinense* vs *H. pantholopsum*) through this approach, and all 54 DEPs were identified as acidic proteins with isoelectric points (pI) ranging from 4.38 to 6.72 (Table 1). Among these, four core stress-responsive DEPs were explicitly characterized, each corresponding to 3 distinct differential spots: heat shock protein cognate 72 (HSC72), PREDICTED: 60 kDa heat shock protein, mitochondrial-like (HSP60), PREDICTED: protein disulfide-isomerase A3-like (PDI A3-like), and albumin. Additionally, MALDI-TOF MS-based analysis provided detailed molecular characteristics of the DEPs:two clusters with high-enrichment abundances of ~60–70 kDa and ~20–30 kDa proteins were visible in the protein profile (Fig. 3-A). The enrichment of stress-responsive proteins (heat shock proteins) in these clusters was verified by targeted analysis. proteins with 2 matched peptides were the most abundant (18 proteins), followed by those with 3 peptides and 4 peptides (Fig. 3-B), indicating high efficiency in protein identification (Käll *et al.,* 2007).The coverage of a protein reflects the extent to which it has been identified, with higher coverage being more advantageous for interpreting features such as protein isoforms (Bumpus *et al.*, 2009), most DEPs exhibited a sequence coverage of 10-30%, with nearly no proteins exceeding 30% coverage (Fig. 3-C).

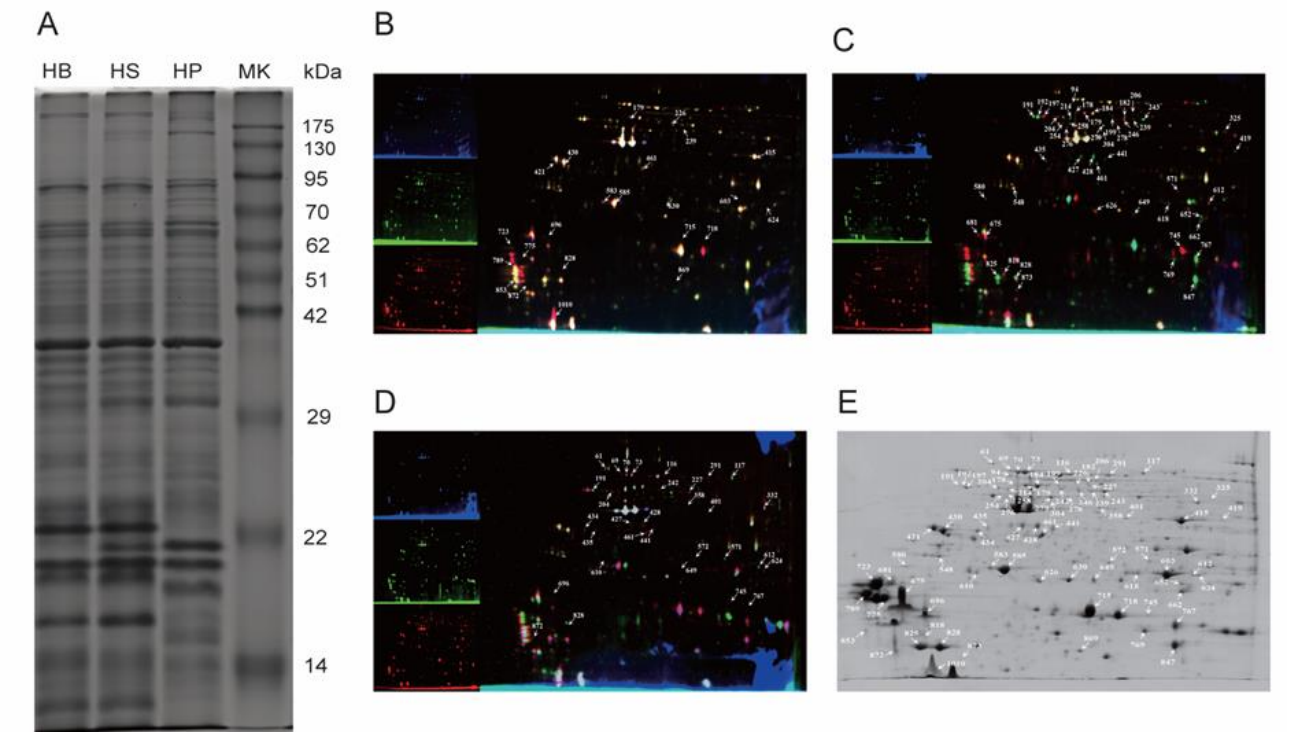

Fig. 2: Proteomic analysis of three *Hypoderma* species was performed using SDS-PAGE and 2D-DIGE. (A) HB = *Hypoderma bovis*, HS = *Hypoderma sinense*, HP = *Hypoderma pantholopsum*, MK = Molecular Weight Marker. (B) HB vs HS, (C) HB vs HP, (D) HS vs HP, (E) integrated overview across all three *Hypoderma* species.

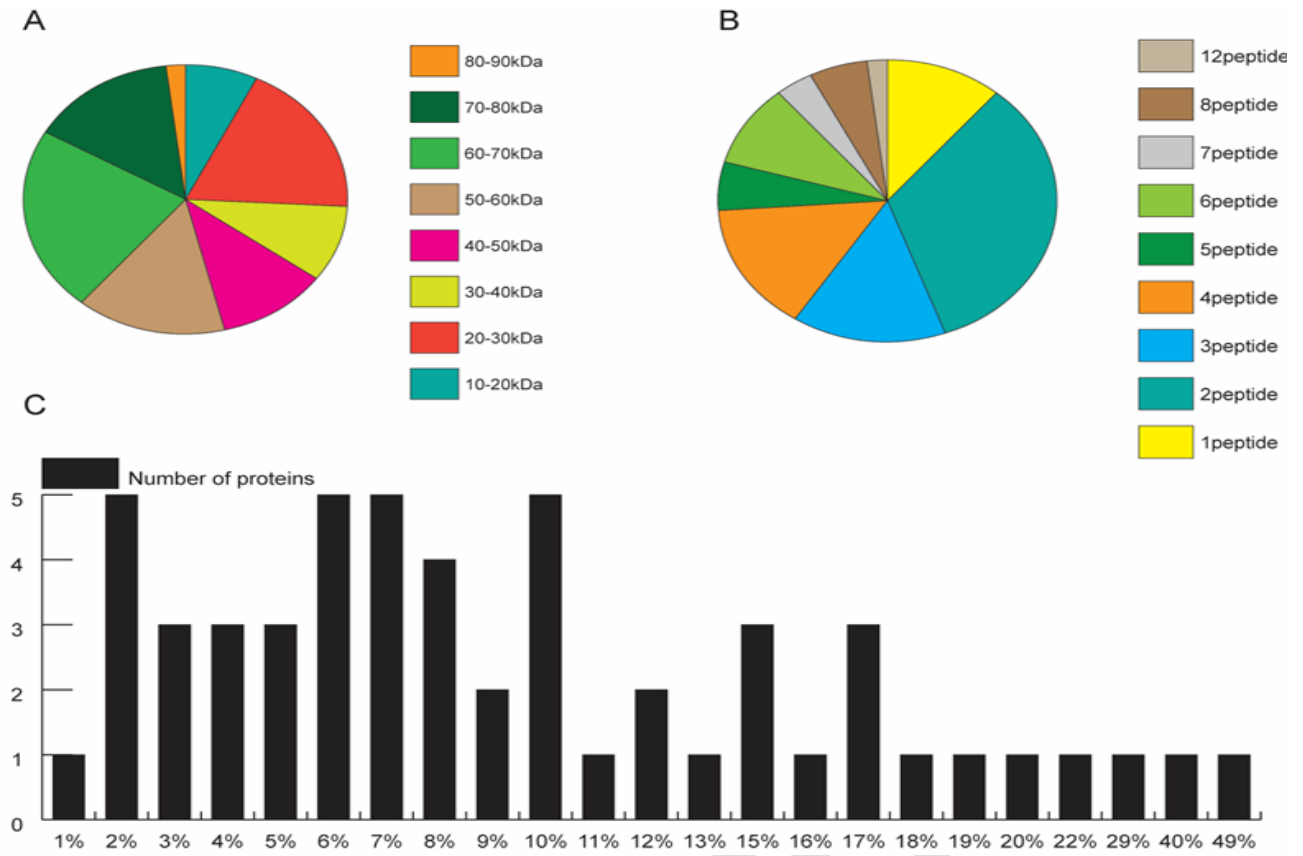

Fig. 3: Differential proteins: peptide mapping, coverage, and molecular weight. (A) Relative molecular mass of differentially expressed proteins, (B) Peptide distribution of differentially expressed proteins, (C) Protein coverage of differentially expressed proteins.

Table 1: Differential protein mass spectrometry results

Spots No	Ac. no.b	Category and name (TOF/TOF sequence) c	pI
69	gi|157658	heat shock protein cognate 72	5.24
70	gi|157658	heat shock protein cognate 72	5.3
73	gi|157658	heat shock protein cognate 72	5.34
178	gi|557759351	PREDICTED: 60 kDa heat shock protein, mitochondrial-like	5.28
179	gi|557759351	PREDICTED: 60 kDa heat shock protein, mitochondrial-like	5.36
184	gi|557759351	PREDICTED: 60 kDa heat shock protein, mitochondrial-like	5.45
239	gi|557753487	PREDICTED: protein disulfide-isomerase A3-like	5.85
243	gi|557753487	PREDICTED: protein disulfide-isomerase A3-like	5.94
246	gi|557753487	PREDICTED: protein disulfide-isomerase A3-like	5.77
427	gi|229552	Albumin	5.34
428	gi|229552	Albumin	5.45
441	gi|229552	Albumin	5.58

Proteomic characterization of *Hypoderma* larvae reveals metabolic process dominance and cytoplasmic protein enrichment: Quantitative image analysis showed that a total of 81 spots to be reproducibly and significantly ($P<0.05$) altered in intensity by more than 1.2-fold. In the three groups, only 2 spots (2.5%) were shared; 15 spots (18.5%) were specific to HB/HS, 2 spots (2.5%) were shared between HB/HS and HB/HP, and 3 spots (3.7%) were shared between HB/HS and HS/HP; 33 spots (40.7%) were specific to HB/HP, 15 spots (18.5%) were specific to HS/HP, and 11 spots (13.6%) were shared between HB/HP and HS/HP only (Fig. 4-A). There were 20, 19, and 11 upregulated spots as well as 2, 29, and 20 downregulated spots in the HB/HS, HB/HP, and HS/HP groups, respectively (Table 2). The protein expression profiles showed distinct regulation patterns across comparative groups: In the HB/HS comparison, relative to HB, proteins 718 and 775 exhibited extreme upregulation in HS, while proteins 226 was significantly downregulation. Where the expression difference for each protein was examined, proteins 197 and 745 showed sharp increases in expression in HPs compared to HBs; protein 825 was downregulated. In the HS/HP comparison, proteins 610 and 745 were drastically upregulated in the HPs, whereas protein 696 was significantly downregulated compared to the HSs.

Table 2: Summary of upregulated and downregulated proteins

HB/HP			HS/HP			HB/HS		
Master No.	T-test	Av. Ratio	Master No.	T-test	Av. Ratio	Master No.	T-test	Av. Ratio
197	0.00035	30.57	610	0.011	43.6	226	0.0017	-1.7
745	0.0061	73.27	696	0.014	-16.51	718	0.000011	42.44
825	0.0044	-14.21	745	0.00077	57.58	775	0.0083	6.84

Functional annotation of proteins was carried out using Blast2GO v2.5 software (Kumar, 2025), grouping them into three major Gene Ontology (GO) classes: Molecular Function, Biological Process, and Cellular Component (Fig. 4-B) (Gene Ontology Consortium *et al.,* 2023). In total, 494 annotations were assigned to 41 functional subcategories. The majority of the unigenes showed a high frequency of Biological Process (BP) with 262 annotations distributed in 22 subcategories. More precisely, cellular process (30 entries) and metabolic process (30 entries) were the most highly represented terms within the BP category. Cellular Component annotations were the second most abundant class, consisting of 166 entries distributed into 11 subcategories, with the most frequent terms being cell (31 entries) and cell part (31

entries). Finally, Molecular Function represented the class with the fewest number of annotations, 66 entries in 8 subcategories, where binding, with 26 entries, and catalytic activity, with 25 entries, were the most highly represented functional attributes. The dominance of cellular and metabolic processes reflects the adaptive strategy of *Hypoderma* larvae in response to high-altitude stress. Rapid cell proliferation and metabolic activity are essential for larval development, and environmental stress further enhances the activation of stress-responsive pathways, including those involved in energy production and antioxidant defense (Hou *et al.*, 2010). Additionally, the enrichment of molecular functions such as binding and catalytic activity suggests that differentially expressed proteins primarily engage in substrate recognition and enzymatic catalysis, which are central to the organism's stress response mechanism (Cui *et al.*, 2010).

Functional annotation with the COG (https://www.ncbi.nlm.nih.gov/research/COG) database resulted in 37 classified entries distributed among 11 subcategories (Fig. 4-C) (Galperin *et al.,* 2021). It is important to mention that the posttranslational modification, protein turnover, and chaperones category (O) was represented by the highest number, with 16 entries. In contrast, five functional categories-lipid transport and metabolism (I), translation/ribosomal structure and biogenesis (J), secondary metabolites biosynthesis/transport/catabolism (Q), general function prediction (R), and signal transduction mechanisms (T)-were represented by the smallest number, with only one entry each. The other categories have intermediate numbers, ranging from 2 to 5 entries per subcategory (Koonin *et al.,* 2004). The elevated representation of Class O (encompassing post-translational modifications, protein turnover, and chaperone activity) underscores the importance of protein quality control mechanisms in high-altitude adaptation. Under high-altitude stress conditions, such as hypoxia and cold exposure, protein denaturation and misfolding are triggered, leading to the activation of molecular chaperones (e.g., heat shock proteins, HSPs) and proteolytic pathways (including the endoplasmic reticulum-associated degradation, ERAD, system) to eliminate misfolded proteins and inhibit the formation of cytotoxic aggregates.

Subcellular localization analysis using Swiss-Prot (2018_04) disclosed the obvious distribution of 41 identified proteins (Fig. 4-D). The cytoplasmic compartment (Cytoplasmic) showed the highest representation with 17 proteins (41.46%), followed by extracellular (Extracellular, 7 proteins; 17.07%) and nuclear (Nuclear, 6 proteins; 14.63%) localizations. On the other hand, lysosomal localization (Lysosomal) constituted the least represented category with only 2 proteins (4.88%). The remaining proteins were distributed between mitochondrial (Mitochondrial, 4 proteins; 9.76%) and endoplasmic reticulum (ER, 5 proteins; 12.20%) compartments (Lundberg and Borner, 2019).The high proportion of differentially expressed proteins in the cytoplasm is consistent with its functional annotations (metabolism and protein folding), as the cytoplasm is the primary site for cellular metabolism and protein synthesis. Heat shock proteins (HSPs) and metabolic enzymes in the cytoplasm can rapidly respond to stress signals, maintaining cellular homeostasis.

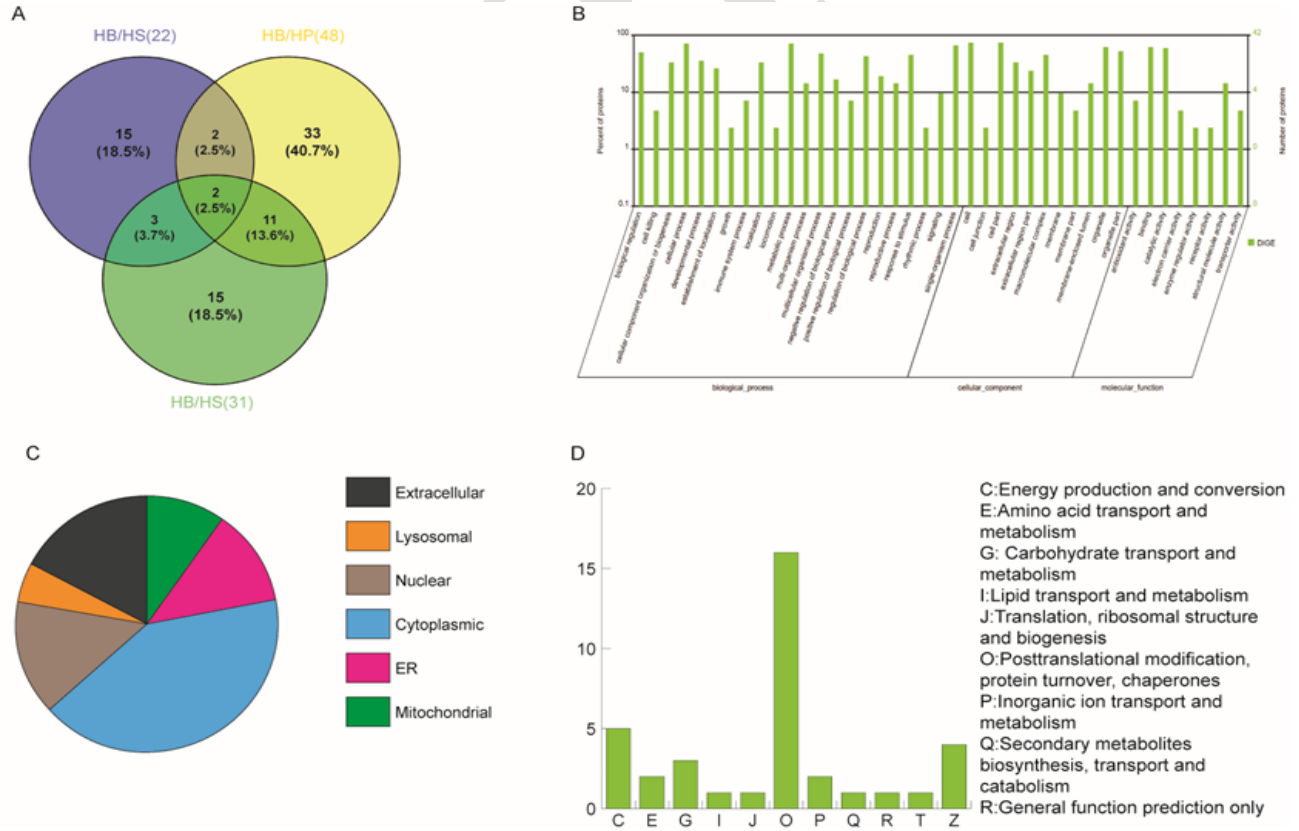

Fig. 4: Statistical and functional analysis of differentially expressed proteins. (A) Differentially Expressed Proteins by Venn Diagram(B) Gene Ontology (GO) functional annotation of differentially expressed proteins, (C) Clusters of Orthologous Groups (COG) classification of differentially expressed proteins, (D) Subcellular localization analysis of differentially expressed proteins.

Protein Analysis of Heat Shock Protein Cognate 72: Four proteins showed the highest abundance in previous experiments. Among these, albumin was excluded because of unclear protein sequence detection results. Further investigations therefore focused on the following three proteins: heat shock protein cognate 72, 60 kDa heat shock protein (mitochondrial-like), and protein disulfide-isomerase A3-like. This study mainly analyzes heat shock protein cognate 72 (HSC72).

The secondary structure of HSC72 was analyzed using Psipred-4.0 online software (Jones, 1999), with results presented in Fig. 5-A. The structure was found to comprise multiple random coils and 20 α-helices. Deep TMHMM prediction (Fig. 5-B) (Almagro Armenteros *et al.,* 2019b) indicated that HSC72 adopts a Globular + SP conformation localized extracellularly. Subsequent tertiary structure prediction via use SWISS-MODEL (Waterhouse *et al.,* 2018) (Fig. 5-C), it demonstrated distinct secondary structural elements represented by geometric shapes.

The electrostatic potential of the three-dimensional structure (by PyMOL software) shows the distribution of charges (Fig. 5-D; red: negative potential, blue: positive potential). STRING-12.0 (Szklarczyk *et al.*, 2023) analysis of Hsc70-3 (98.8% sequence similar to HSC72), showing 10 highly reliable interactors with a confidence score > 0.9, including: Gp93, CG2918, Manf, Hsp83, Sil1, Calr, Ire1, shv, Sec63, and Der-1, are presented in Fig. 5-E and Table 3. This interaction network indicate the possibility of involvement in molecular complexes or signaling pathways.

Table 3: Functional annotation of Heat shock cognate 72 interacting proteins

Protein Identifier	Annotation
Gp93	Glycoprotein 93 (Gp93) encodes a heat shock protein Hsp90 family member that is involved in midgut development.
CG2918	EG:25E8.1 protein; It is involved in the biological process described with: multicellular organism reproduction
Manf	Mesencephalic astrocyte - derived neurotrophic factor (Manf) encodes an evolutionarily conserved neurotrophic factor.
Hsp83	Heat shock protein 83; Molecular chaperone that promotes the maturation
Sil1	Nucleotide exchange factor Sil1; Required for protein translocation and folding in the endoplasmic reticulum (ER).
Calr	Calreticulin; Molecular calcium - binding chaperone promoting folding
Ire1	Inositol - requiring enzyme - 1 (Ire1) encodes a transmembrane protein that mediates the unfolded protein response
shv	DnaJ homolog shv; Maintains stem cell niche architecture in the testes.
Sec63	Secretory 63; Protein transmembrane transporter activity; RNA binding.
Der-1	Derlin - 1; May be involved in the degradation process of specific misfolded endoplasmic reticulum (ER) luminal proteins.

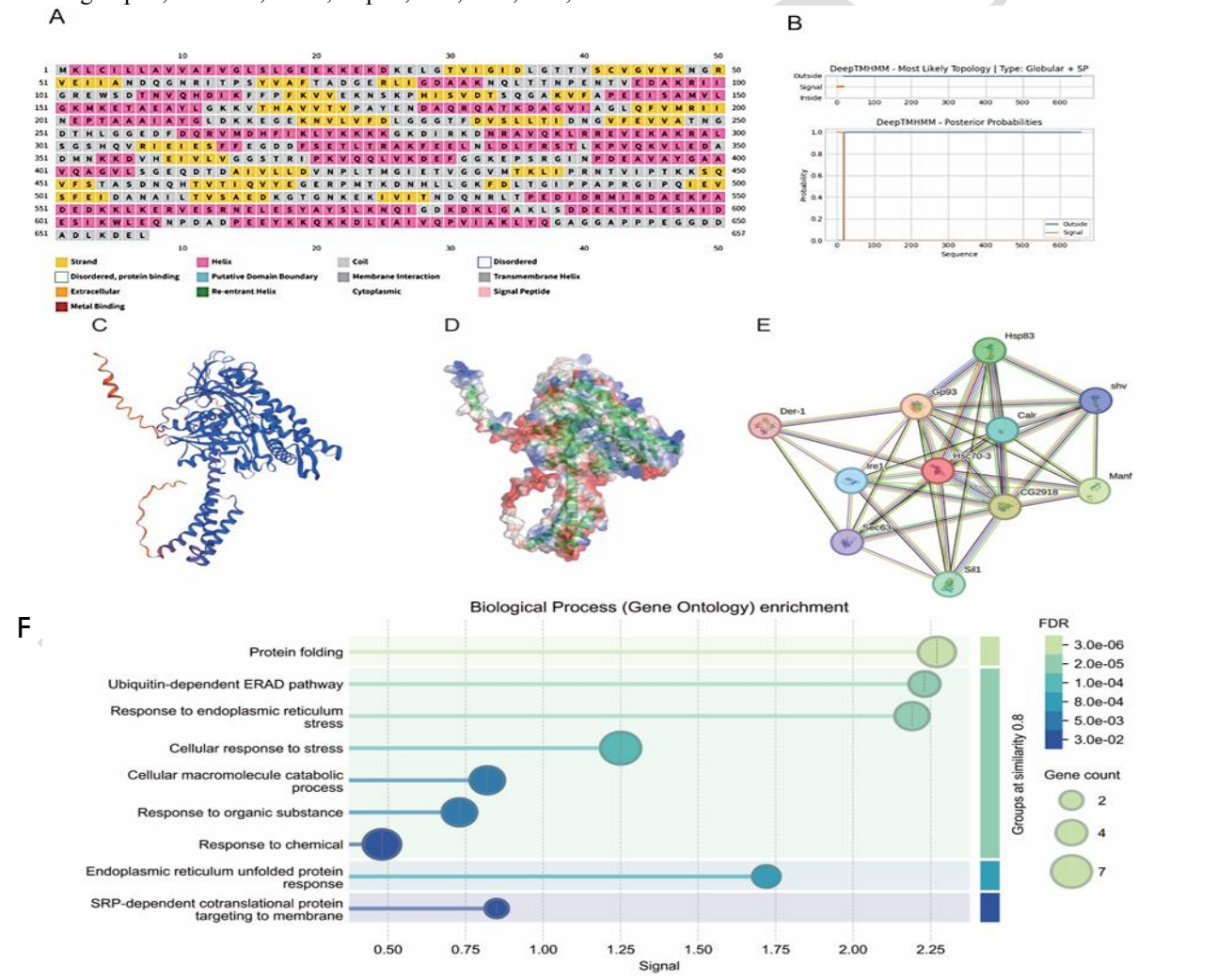

Fig. 5: Analysis of heat shock cognate 72 protein. (A) Secondary structure of Heat Shock Cognate 72; (B) Transmembrane domain prediction of heat shock protein cognate 72 using DeepTMHMM; (C) Tertiary structure of heat shock protein cognate 72; (D) Electrostatic potential surface analysis of heat shock protein cognate 72; (E) Interaction network of T1PA52_MUSDO (heat shock protein cognate 72 ortholog) with partner proteins; (F) Functional annotation of heat shock protein cognate 72-related proteins.

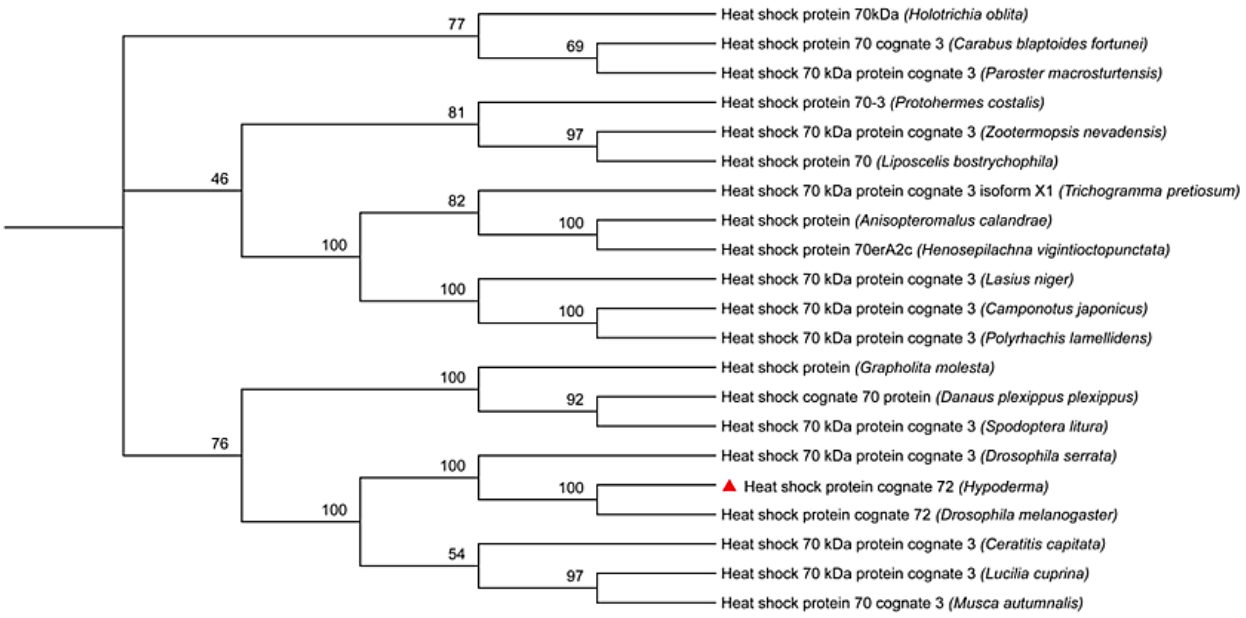

Fig. 6: Phylogenetic tree analysis of heat shock cognate 72 across multiple species.

The GO analysis showed a significant association with "Protein folding" and "Ubiquitin-dependent ERAD pathway" (Figure 5-F, false discovery rate FDR<0.05), because HSC72 may exert a key chaperone function during development through its molecular scaffold activity.

After the sequence of HSC72 by sequencing, we aligned this sequence with non-redundant homologous sequences using the Clustal W algorithm in MEGA software. To ensure the accuracy and biological relevance of the alignment results, the research team finely optimized the relevant alignment parameters. The finally constructed phylogenetic tree (Figure 6) revealed that HSC72 is a constitutively expressed member (non-stress-inducible) of the HSP70 superfamily, participating in processes such as protein folding, transport, and misfolded protein repair in cells.

Phylogenetic analysis results showed that *Hypoderma* belonged to the evolutionary clade with the highest support (bootstrap value = 100), have *Drosophila serrata* (*D. serrata*) and *Drosophila melanogaster* (*D. melanogaster*) the HSC72 protein have remarkable sequence conservation, this is a pattern common to housekeeping genes under severe functional constraint. We think that the conservation results from the crucial role about HSC72 plays in processes such as stress management and embryogenesis, which have persisted since these dipteran lineages diverged.

DISCUSSION

In order to examine molecular reactions to external stress of three species of *Hypoderma* larvae (*H. bovis*, *H. pantholopsum*, and *H. sinense*), the protein expression profiles of them were identified. The high-altitude environment, marked by hypoxia, cold temperatures, and elevated ultraviolet radiation, imposes significant stress on cellular homeostasis. Notably, all 54 differentially expressed proteins (DEPs) identified in this context are acidic, with isoelectric points spanning from 3.78 to 6.76. This enrichment of acidic proteins reflects an adaptive evolutionary mechanism, as acidic proteins tend to be more stable in mildly acidic intracellular compartments, such as stress-induced lysosomes, and retain structural integrity under cold stress. Moreover, the acidic nature of these proteins likely enhances charge-mediated protein-protein interactions, which are crucial for forming stress response complexes, such as those involving heat shock protein chaperones. Key stress response proteins, including Heat Shock Cognate 72 (HSC72), 60 kDa Heat Shock Protein (HSP60), and Protein Disulfide Isomerase A3-like (PDI A3-like), are among these acidic DEPs and are instrumental in processes such as oxidative damage repair, protein folding, and redox homeostasis—functions vital for survival in high-altitude conditions.

Notably, targeted identification of these differentially expressed proteins (DEPs) heavily relied on MALDI-TOF MS, which has the capability of precisely characterizing protein identity, isoelectric point (pI), and molecular weight from the excised 2D-DIGE spots. By MALDI-TOF MS with MASCOT database search, a total of 54 acidic DEPs with pI ranging between 4.38 and 6.72 were confirmed across the three *Hypoderma* species. These include the core stress-responsive proteins such as heat shock protein cognate 72 (HSC72), 60 kDa heat shock protein (HSP60), and protein disulfide-isomerase A3-like (PDI A3-like), with each being verified with three distinct differential spots (Table 1). The HSP family, evolutionarily conserved molecular chaperones, was significantly enriched (fold change > 3.0, P<0.01) and presumably suits cellular repair demands under salt-induced stress (Vu *et al.*, 2023). PDI, a critical mediator of the proper formation of disulfide bonds and redox homeostasis, demonstrated coordinated upregulation that could mitigate oxidative damage through the maintenance of enzymatic activity (Ali Khan and Mutus, 2014). Albumin, a multifunctional transport protein, showed species-specific expression patterns and may putatively serve ion shuttling or osmoregulation roles. These molecular signatures are strikingly like the previously reported conserved stress adaptation mechanisms in extremophilic arthropods (Kültz,

2005). Species-specific proteomic heterogeneity was represented, such that only 2 of the differentially expressed proteins were shared among all three groups, whereas 40.7% of the DEPs in HB/HP comparison were unique (Fig. 4). The high proportion of unique DEPs in HB/HP likely reflects specialized molecular adaptations that *H. pantholopsum* has evolved to cope with these harsher conditions, while the minimal shared DEPs (only 2) suggest that each species has developed distinct proteomic strategies to navigate their respective ecological niches.

As shown in Fig. 3, the proteomic analysis showed that the identified peptides contained 2–8 matched fragments, and half of the differential proteins exhibited sequence coverage between 10% and 30%. The low coverage is likely due to technical limitations in terms of protein abundance, digestion efficiency, and mass spectrometry parameter optimization. In addition, improved sample preparation methods and new-generation platforms, such as Orbitrap Fusion Lumos, are required in further investigations (Michalski *et al.,* 2011).

The molecular weight distribution of detected proteins was from 10 to 90 kDa, which corresponded with the established characteristic of insect proteomes. There were two clusters of molecular mass showing high abundance: 60–70 kDa and 20–30 kDa (Fig. 3). These peaks probably correspond to the enrichments of stress-responsive proteins, including heat shock proteins (HSP60, HSP70, HSPB1) (De Maio *et al.,* 2019; He *et al.,* 2010; Teng *et al.,* 2019) and protein disulfide-isomerase A3-like isoforms, known mediators of environmental stress adaptation in arthropods (Watanabe, Laurindo, and Fernandes, 2014).

Though the study systematically elucidated the proteomic characteristics of botfly larvae under environmental stress, but have some limitations remain: the mass spectrometry coverage was relatively low, probably missing low-abundance or membrane proteins; in addition, some functional annotations is ambiguous and need to be integrated with genomic or metabolomic analysis for refinement. Further studies should work on optimizing sample pretreatment techniques and use high-sensitivity mass spectrometry platforms such as Orbitrap to improve the detection depth, so that can comprehensively explaining the adaptation mechanisms of *Hypoderma* larvae. Future studies could employ multi-omics integration (e.g., metabolomic-proteomic analyses) to uncover novel functional proteins(Lei *et al*., 2023). According to the structural analysis, HSC72 has an architecture composed of 20 α-helices and random coils. This structural scaffold is essential for its chaperone activity. Potential involvement in extracellular signaling was indicated by DeepTMHMM's prediction of an extracellular globular domain with a signal peptide. Different charge distributions that probably govern protein-protein interactions were found by examining the tertiary structure and electrostatic surface. A coordinated mechanism in protein quality control is suggested by the network placement of HSC72 within a complex that also includes Gp93, CG2918, and Hsp83. This role is supported by strong functional enrichment for "Protein folding" and the "Ubiquitin-dependent ERAD pathway" (FDR < 0.05). We thus conclude that during *Hypoderma* development, HSC72 functions as a molecular scaffold to prevent cytotoxic aggregation of nascent polypeptides. Additionally, it likely contributes to ERAD-mediated degradation of misfolded proteins, working in concert with its interaction partners to maintain proteostasis under environmental stress.

Phylogenetic analysis shows that *Hypoderma* sp. and *Drosophila melanogaster* HSC72 sequences represent a monophyletic clade with maximal bootstrap support (100%; Fig. 6), reinforcing the concept that phylogenetic distance underlies protein sequence conservation. Since both dipteran species have evolutionarily conserved needs for intracellular proteostasis in their development-specifically, cellular remodeling and protein folding during complete metamorphosis-their HSC72 sequences retain important functional domains due to purifying selection.

In the phylogeny, *Hypoderma* and *Drosophila melanogaster* HSC72 sequences clustered have 100% bootstrap support (Fig. 6), it evidences that phylogenetic relationships drive protein sequence conservation. Because both dipteran species have evolutionarily conserved needs about intracellular proteostasis in their development-specifically, cellular remodeling and protein folding during complete metamorphosis-their HSC72 sequences retain important functional domains because of purifying selection.

Within the HSP70 superfamily, HSC72 is a constitutively expressed homolog (non-stress-inducible but constantly active in protein folding, translocation, and misfolding repair) that evolves under strong functional constraints. Thus, mutations in its critical functional domains would disrupt cellular proteostasis and be purged by selection. These constraints impose sequence conservation across phylogenetically closely related species, thus establishing a co-evolutionary coupling between taxonomic affinity and molecular conservation patterns.

Though the study systematically elucidated the proteomic characteristics of *Hypoderma* larvae under environmental stress, but have some limitations remain: the mass spectrometry coverage was relatively low. This issue stems from two main factors: first, low-abundance functional proteins (such as signaling pathway regulators) within *Hypoderma* larvae tissues are prone to loss or degradation during extraction and isolation; second, membrane and hydrophobic proteins are difficult to resolve via conventional 2D-DIGE and mass spectrometry due to their low solubility. Further studies should work on optimizing sample pretreatment techniques and use high-sensitivity mass spectrometry platforms such as Orbitrap to improve the detection depth (Singh *et al.*, 2021), so that can comprehensively explain the adaptation mechanisms of *Hypoderma* larvae.

Conclusions: This study provides the first comprehensive comparative proteomic analysis of three *Hypoderma* larvae species (*H. bovis*, *H. sinense*, and *H. pantholopsum*) from the high-altitude Qinghai-Tibet Plateau. Our integrated proteomic approach identified 1,031 proteins, 54 of which were significantly differentially expressed acidic proteins conserved across the three *Hypoderma* species. The key findings reveal that the molecular adaptation strategies of these parasites are centered on fundamental metabolic and cellular stress responses. Proteins such as heat shock proteins (HSC72, HSP60), protein disulfide isomerase (PDI A3-like), and albumin were consistently identified,

underscoring their critical roles in mitigating oxidative damage, maintaining protein homeostasis (proteostasis), and facilitating ion transport.

A striking level of proteomic heterogeneity was observed among the species. Only two differentially expressed proteins were common to all three, while a substantial proportion (41.5%) were unique to the comparison between *H. bovis* and the high-altitude endemic species, *H. pantholopsum*. This suggests that *H. pantholopsum* has evolved distinct molecular adaptations, including the upregulation of energy metabolism and protein homeostasis pathways, to cope with extreme environmental stressors. The functional annotation confirmed that the differentially expressed proteins are predominantly involved in "cellular processes" and "metabolic processes" (Biological Process), and "binding" and "catalytic activity" (Molecular Function). Furthermore, in-depth structural and phylogenetic analysis of HSC72 highlighted its essential, evolutionarily conserved chaperone functions in protein folding and the ubiquitin-dependent ERAD pathway, which are crucial for larval development and stress resilience.

In summary, this work elucidates the critical molecular mechanisms underlying high-altitude adaptation in *Hypoderma* species. It delivers valuable insights into the molecular ecology of these economically significant parasites and establishes a foundational proteomic resource for informing future targeted strategies for the control of hypodermiasis on the Qinghai-Tibet Plateau.

Funding: This work was supported by grants from the National Natural Science Foundation of China (32560866), the Key R&D and Conversion Plan of Qinghai Province (2025-QY-227), the Open Project of State Key Laboratory for Diagnosis and Treatment of Severe Zoonotic Infectious Diseases (RCGHCRB202506), and the Qinghai Province "Kunlun Talents High-end Innovation and Entrepreneurial Talents" Talent Training Project.

Acknowledgements: We thank all of the veterinarians for aiding in sample collection. The authors extend their appreciation to the "Ongoing Research Funding Program" (ORF-2025-191), King Saud University, Riyadh, Saudi Arabia.

Competing interests: The authors declare no competing interests.

Author's contribution: YF: Conceptualization, Project administration, Data analysis, Manuscript drafting; SW: Executing laboratory experiments, Data analysis, Manuscript drafting; ZL, RM, HD, XZ, XS, JL, YL, DC, XZ, MHA and WC: Sample collection, Environmental data collection, Data analysis, Review & Editing; All authors read and approved the final manuscript.

REFERENCES

Ali Khan H and Mutus B, 2014. Protein disulfide isomerase a multifunctional protein with multiple physiological roles. Front Chem 2:70.

Almagro Armenteros JJ, Salvatore M, Emanuelsson O, *et al.*, 2019a. Detecting sequence signals in targeting peptides using deep learning. Life Sci Alliance 2:e201900429.

Almagro Armenteros JJ, Tsirigos KD, Sønderby CK, *et al.*, 2019b. SignalP 5.0 improves signal peptide predictions using deep neural networks. Nat Biotechnol 37:420-423.

Bendtsen JD, Jensen LJ, Blom N, *et al.*, 2004. Feature-based prediction of non-classical and leaderless protein secretion. Protein Eng Des Sel 17:349-356.

Blum M, Chang H-Y, Chuguransky S, *et al.*, 2021. The InterPro protein families and domains database: 20 years on. Nucleic Acids Res 49:D344-D354.

Bumpus SB, Evans BS, Thomas PM, *et al.*, 2009. A proteomics approach to discovering natural products and their biosynthetic pathways. Nat Biotechnol 27:951-956.

Cairen Z, Tie F and Zhang Y, 2019. Infection status and control effect of bovine hypodermosis in Haiyan County, Qinghai Province. Breed Feed:52-54.

Cui S-J, Xu L-L, Zhang T, *et al.*, 2013. Proteomic characterization of larval and adult developmental stages in Echinococcus granulosus reveals novel insight into host-parasite interactions. J Proteomics 84:158-175.

De Maio A, Cauvi DM, Capone R, *et al.*, 2019. The small heat shock proteins, HSPB1 and HSPB5, interact differently with lipid membranes. Cell Stress Chaperones 24:947-956.

Dowling P, 2023. DIGE Analysis Software and Protein Identification Approaches. Methods Mol Biol 2596:39-50.

Emanuelsson O, Brunak S, von Heijne G, *et al.*, 2007. Locating proteins in the cell using TargetP, SignalP and related tools. Nat Protoc 2:953-971.

Fu Y, Li W, Duo H, *et al.*, 2016. Genetic diversity and population genetics of the warble flies *Hypoderma bovis* and *H. sinense* in Qinghai Province, China. Parasit Vectors 9:145.

Galperin MY, Wolf YI, Makarova KS, *et al.*, 2021. COG database update: focus on microbial diversity, model organisms, and widespread pathogens. Nucleic Acids Res 49:D274-D281.

Gene Ontology Consortium, Aleksander SA, Balhoff J, *et al.*, 2023. The Gene Ontology knowledgebase in 2023. Genetics 224:iyad031.

González S, Del Rio ML, Diez MN, *et al.*, 2023. Identification of *Hypoderma actaeon* (Diptera: Oestridae) in red deer (*Cervus elaphus*) from northern Spain: Microscopy study and molecular analysis. Microsc Res Tech 86:3-11.

Guan Z and Tai Y, 2023. Prevention and control of bovine hypodermosis. Contemp Anim Husb:107-108.

Hassan M, Khan MN, Abubakar M, *et al.*, 2010. Bovine hypodermosis-a global aspect. Trop Anim Health Prod 42:1615-1625.

He S, Yang L, Lv Z, *et al.*, 2010. Molecular and functional characterization of a mortalin-like protein from Schistosoma japonicum (SjMLP/hsp70) as a member of the HSP70 family. Parasitol Res 107:955-966.

Hebert PDN, Cywinska A, Ball SL, *et al.*, 2003. Biological identifications through DNA barcodes. Proc Biol Sci 270:313-321.

Hou Q, Tan Y, Liu Q, *et al.,* 2021. Morphological and molecular identification of hypodermatid flies parasitic on plateau zokors. Chin J Zool 56:432-440.

Hou Y, Zou Y, Wang F, *et al.*, 2010. Comparative analysis of proteome maps of silkworm hemolymph during different developmental stages. Proteome Sci 8:45.

Huang DW, Sherman BT and Lempicki RA, 2009. Systematic and integrative analysis of large gene lists using DAVID bioinformatics resources. Nat Protoc 4:44-57.

Jones DT, 1999. Protein secondary structure prediction based on position-specific scoring matrices. J Mol Biol 292:195-202.

Käll L, Canterbury JD, Weston J, *et al.*, 2007. Semi-supervised learning for peptide identification from shotgun proteomics datasets. Nat Methods 4:923-925.

Koonin EV, Fedorova ND, Jackson JD, *et al.*, 2004. A comprehensive evolutionary classification of proteins encoded in complete eukaryotic genomes. Genome Biol 5:R7.

Kültz D, 2005. Molecular and evolutionary basis of the cellular stress response. Annu Rev Physiol 67:225-257.

Kumar A, 2025. Genome Annotation. Methods Mol Biol 2859:21-37.

Lei J, Gong M and Liu L, 2023. Application of multi-omics analysis in insect diapause. J Environ Entomol 45:899-909.

Li K, Shahzad M, Zhang H, *et al.*, 2018. Socio-economic burden of parasitic infections in yaks from 1984 to 2017 on Qinghai Tibetan Plateau of China—A review. Acta Tropica 183:103-109.

Li T, Xu S-L, Oses-Prieto JA, *et al.*, 2011. Proteomics analysis reveals post-translational mechanisms for cold-induced metabolic changes in Arabidopsis. Mol Plant 4:361-374.

Li W, 2007. Observation of Morphology of Third-instar warble in Yak by Scanning Electron Microscopy. Qinghai J Anim Husb Vet Med:19-20.

Li W, Fu Y, Duo H, *et al.*, 2014. An Epidemiological Study of *Hypoderma* Infection and Control Using Ivermectin in Yaks in Qinghai Province, China. J Vet Med Sci 76:183-188.

Lundberg E and Borner GHH, 2019. Spatial proteomics: a powerful discovery tool for cell biology. Nat Rev Mol Cell Biol 20:285-302.

Ma Y and Geri L, 2017. Research status of Tibetan antelopes (*Pantholops hodgsonii*). Chin J High Alt Med Biol 38:206-212.

Mansuri MS, Bathla S, Lam TT, *et al.*, 2024. Optimal conditions for carrying out trypsin digestions on complex proteomes: From bulk samples to single cells. J Proteomics 297:105-109.

May C, Brosseron F, Chartowski P, *et al.*, 2021. Differential Proteome Analysis Using 2D-DIGE. Methods Mol Biol 2228:77-84.

Michalski A, Damoc E, Hauschild JP, *et al.*, 2011. Mass spectrometry-based proteomics using Q Exactive, a high-performance benchtop quadrupole Orbitrap mass spectrometer. Mol Cell Proteomics 10:M111.011015.

Pan Y, Xiao H, Gao W, *et al.*, 2024. Prevention and Control Strategies for Major Parasitic Diseases of Yaks. China Animal Health 26:27-28.

Qing H, 2022. Comprehensive prevention and control of bovine ectoparasitosis. China Anim Husb:60-61.

Shao F. and Yang X., 2022. Diagnosis and treatment of *Hypoderma bovis* myiasis. Sichuan Animal and Veterinary Sciences, 49: 58.

Singh SA, Andraski AB, Higashi H, *et al.*, 2021. Metabolism of PLTP, CETP, and LCAT on multiple HDL sizes using the Orbitrap Fusion Lumos. JCI Insight 6:e143526, 143526.

Szklarczyk D, Kirsch R, Koutrouli M, *et al.*, 2023. The STRING database in 2023: protein-protein association networks and functional enrichment analyses for any sequenced genome of interest. Nucleic Acids Res 51:D638-D646.

Teng R, Liu Z, Tang H, *et al.*, 2019. HSP60 silencing promotes Warburg-like phenotypes and switches the mitochondrial function from ATP production to biosynthesis in ccRCC cells. Redox Biol 24:101218.

Tsuchida S, Umemura H and Nakayama T, 2020. Current Status of Matrix-Assisted Laser Desorption/Ionization-Time-of-Flight Mass Spectrometry (MALDI-TOF MS) in Clinical Diagnostic Microbiology. Molecules 25:4775.

Vu NT, Nguyen NBT, Ha HH, *et al.*, 2023. Evolutionary analysis and expression profiling of the HSP70 gene family in response to abiotic stresses in tomato (Solanum lycopersicum). Sci Prog 106:36850422148843.

Wang D, Xu B, Sun Y, *et al.,* 2022. Differential analysis of latex proteins and identification of phosphorylated proteins in rubber tree clones PR107 and CATAS8-79. Chin J Trop Crops 43:904-914.

Wang X., 2025. Epidemiology and prevention strategies of *Hypoderma bovis* myiasis in yaks. Northern Animal Husbandry, 37.

Watanabe MM, Laurindo FRM and Fernandes DC, 2014. Methods of measuring protein disulfide isomerase activity: a critical overview. Front Chem 2:73.

Waterhouse A, Bertoni M, Bienert S, *et al.*, 2018. SWISS-MODEL: homology modelling of protein structures and complexes. Nucleic Acids Res 46:W296-W303.

Weigl S, Traversa D, Testini G, *et al.*, 2010. Analysis of a mitochondrial noncoding region for the identification of the most diffused *Hypoderma* species (Diptera, Oestridae). Vet Parasitol 173:317-323.

Zhang W and Chait BT, 2000. ProFound: an expert system for protein identification using mass spectrometric peptide mapping information. Anal Chem 72:2482-2489.

Zhang Y, Lai BS, Juhas M, *et al.*, 2019. *Toxoplasma gondii* secretory proteins and their role in invasion and pathogenesis. Microbiol Res 227:126293.

Zhang Z, Ji L, Li Z, *et al.,* 2014. A case report of human myiasis in Huangzhong District, Qinghai Province. J Med Entomol Control 30:1279-1280.